JOURNAL OF SOLID STATE CHEMISTRY 60, 139–144 (1985)

Proton Motion in $HNbO_3$ and $HTaO_3$

M. T. WELLER AND P. G. DICKENS*

Inorganic Chemistry Laboratory, South Parks Road, Oxford OX1 3QR, United Kingdom

Received September 17, 1984; in revised form April 22, 1985

Proton NMR relaxation times T_1, $T_{1\rho}$, and T_2 are reported for the compounds $HTaO_3$ and $HNbO_3$ in the temperature range 170–540 K. The data show that for both compounds two types of motion occur. Proton diffusion occurs in both compounds above 400 K with a correlation time, τ_c^0, of ~30 ps and an activation energy of ~50 kJ mole^{-1}, approximately twice that for the localized process occurring at lower temperatures. Alternating current conductivity measurements have been used to study proton diffusion above 470 K in these compounds.

Introduction

The materials $HTaO_3$ and $HNbO_3$ obtained by ion exchange of $LiMO_3$ (M = Ta,Nb) (*1*) are white crystalline solids of cubic symmetry. Their basic X-ray patterns suggest that they are isomorphous with H_xWO_3 (*2*) and H_xReO_3 (*3*) and work by Fourquet and co-workers has confirmed this interpretation following a powder neutron diffraction study of $HNbO_3$ (*4*). A recent study by the authors on $HTaO_3$ using powder neutron diffraction confirms a similar structure for this material (*5*). This work demonstrated that these materials may be described as oxyhydroxides, consisting of $M(O,OH)_6$ octahedra sharing vertices as in the ReO_3 structure. Broad line NMR measurements below room temperature for $HNbO_3$, (*4*), indicated a presumed short range motion with characteristic parameters E_a = 4.8 kJ mole^{-1} and $\tau_c^0 = 10^{-7}$ s. Below 150 K the experimental second moment was found to be constant, $M_2 = 10$ G^2, and this was interpreted in terms of the formation of some —OH_2 groups within the structure.

NMR studies of the isostructural compounds H_xWO_3 (*6*) and H_xReO_3 (*7*) have shown proton motion to occur above room temperature via a mechanism characterized by the parameters $E_a \sim 14$ kJ mole^{-1} and $\tau_c^0 \sim 10^{-7}$ s. For these compounds contributions to the relaxation process may arise from paramagnetic centers and conduction band electrons since both are metallic.

In the present work proton motion in $HNbO_3$ and $HTaO_3$ has been studied by pulsed solid-state NMR in the range 150–520 K. We also report a.c. conductivity measurements taken in the range 470–570 K for both compounds.

Experimental Methods

Materials

Samples of HMO_3 were obtained from $LiNbO_3$ and $LiTaO_3$ by ion exchange. $LiMO_3$ was prepared from M_2O_5 and dry

* To whom correspondence should be addressed.

0022-4596/85 $3.00

Li_2CO_3 by heating a stoichiometric mixture at 900°C for 24 h. Powder X-ray diffraction showed the products to be pure.

$HNbO_3$

Samples were prepared by stirring ~5 g of $LiNbO_3$ with 150 ml of 3 *M* HNO_3 at 90°C for 5 days. The pure white crystalline product was then filtered off and washed with copious amounts of distilled water until all traces of acid were removed. The crystalline solid was then dried at 120°C for 24 h. Powder X-ray diffraction of the product showed a pure cubic phase of $HNbO_3$ with refined lattice parameter of a = 7.6442[8] Å, (a = 7.645 Å (*1*)).

$HTaO_3$

Exchange of lithium ions in $LiTaO_3$ requires more forcing conditions than the corresponding niobium compound. A sample of $LiTaO_3$ was stirred with 9 *M* H_2SO_4 at 110°C for 7 days. The product was isolated in a similar manner to that of $HNbO_3$. Powder X-ray diffraction patterns of the product showed a pure cubic phase with a = 7.6225[9] Å, (a = 7.620 Å (*1*)).

Samples were decomposed thermogravimetrically to M_2O_5 and H_2O by heating to 700°C. Weight loss over this range indicated compositions of $H_{0.98\pm0.02}NbO_3$ and $H_{1.00\pm0.02}TaO_3$.

NMR Studies

Equipment

The ^1H NMR relaxation times T_1, $T_{1\rho}$, and T_2 were measured in the temperature range 170 K < T < 540 K using a Bruker SXP spectrometer operating at $\omega_0 = 2\pi \times$ 20 or 60 MHz and Datalab signal-averaging equipment. T_1 was measured above 250 K with a 180_x–τ–90_x sequence, and below 250 K by a multiple-pulse saturation method. $T_{1\rho}$ was measured using the method of Hartmann and Hahn (*8*) (with B_1 = 11.7 or 4.70 G). T_2 was measured from free induction decays or at the highest temperatures by the Carr–Purcell–Meiboom–Gill pulse sequence (*9*); low temperature values were also recorded using the zero time resolution technique (*10*).

Alternating Current Conductivity

Conductivity measurements were carried out over the frequency range 10^{-4}–10^6 Hz using a Solartron 1170 Impedance Analysis System. The temperature range studied was 470–570 K. The cell assembly comprised of 13-mm diameter discs of material compressed under 5 tons. The surface of the disc was coated with platinum and it was then mounted between two gold electrodes and light pressure applied by means of a clamp to ensure good interfacial contact. A typical impedance plane plot is shown in Fig. 1.

Results

The relaxation times T_1, $T_{1\rho}$, and T_2 plotted against $1/T$ are shown in Fig. 2 for $HNbO_3$ and Fig. 3 for $HTaO_3$. Second moments were calculated from the curvature of the solid-echoes at their maxima, with values of 9.1 G^2 for $HNbO_3$, and 5.2 G^2 for $HTaO_3$ at the lowest temperatures investigated. This technique is of comparable accuracy to continuous wave methods (*11*). The temperature dependence of conductivity derived from the a.c. conductivity measurements is shown in Fig. 4.

Discussion

It is possible to account for the relaxation behavior by assuming that in both compounds two types of proton motion occur. The high-temperature relaxation behavior for both compounds, where $T_2 \sim T_{1\rho}$ and T_2 is increased by 2 orders of magnitude above the rigid lattice value, provides strong evi-

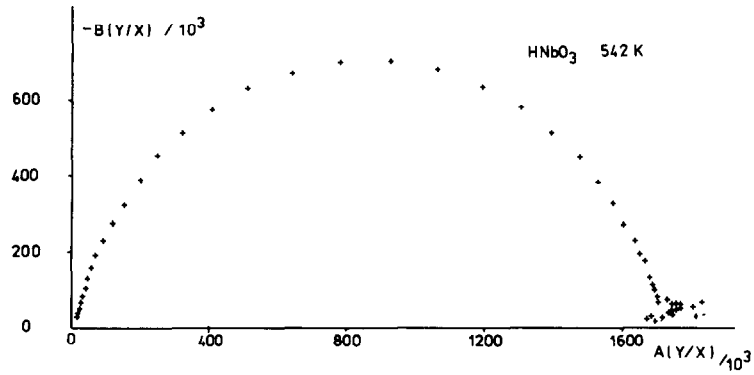

FIG. 1. Impedance plane plot from a.c. conductivity measurements on $HNbO_3$ at 542 K.

dence for translation (self-diffusion) involving hydrogen atoms. Such a diffusive motion modulates the T_2 data above 380 K and will be designated Motion A. A second motion which affects the T_2 data in the range 200–310 K will be denoted Motion B. All data can be interpreted using BPP theory provided account is taken of the presence of both relaxation processes.

$HNbO_3$

Assuming the validity of BPP theory (*12*) for this system and provided τ_c conforms to the relationship

$$\tau_c = \tau_c^0 e^{E_a/RT}$$

the theory predicts that for a plot of $\log_{10}T_1$ verses $1/T$ the limiting slope on either side

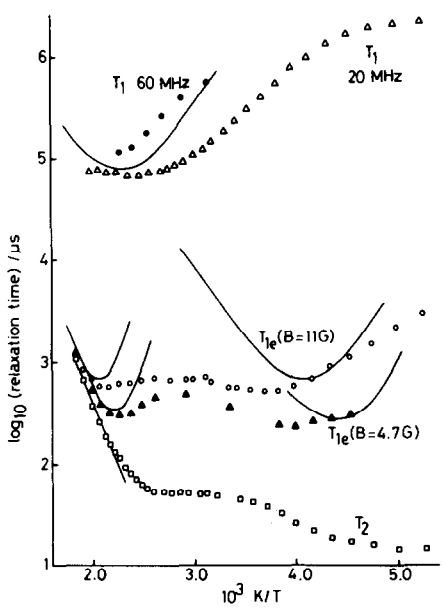

FIG. 2. Temperature dependence of proton relaxation times for $HNbO_3$. Values calculated using BPP theory shown as solid lines.

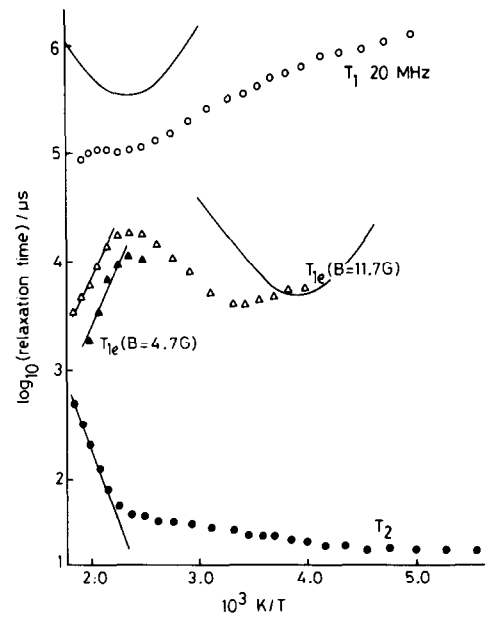

FIG. 3. Temperature dependence of proton relaxation times for $HTaO_3$. Values calculated using BPP theory shown as solid lines.

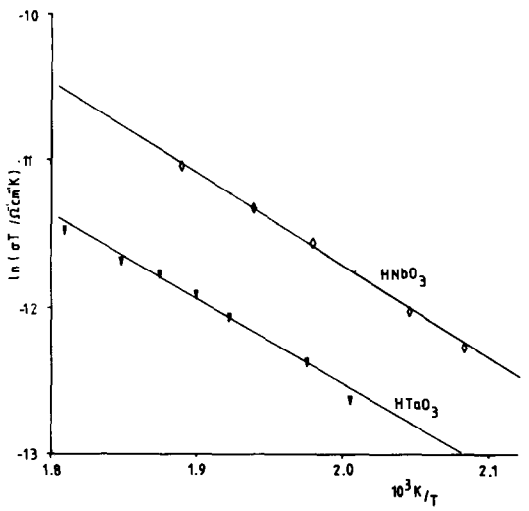

FIG. 4. Temperature dependence of conductivity for $HNbO_3$ and $HTaO_3$.

of a T_1 minimum gives the activation energy E_a for the motion. A value for E_a can also be derived from the variation of T_2 in the line narrowing region.

Motion A

An activation energy was derived for this process from the high temperature T_2 data of 42.6 ± 0.5 and an estimate of 43.1 ± 1.0 kJ mole^{-1} was taken from the $T_{1\rho}$ data (B_1 = 4.7 G) above the minimum. If an exponential correlation function is assumed it is possible to derive a value for the correlation time τ_c^0 using the position of the $T_{1\rho}$ minimum. The value derived using both sets of $T_{1\rho}$ data was 30 ± 10 ps.

Motion B

At low temperatures the weak temperature dependence of T_1 and $T_{1\rho}$ arises because the paramagnetic interaction becomes dominant. The correlation time, τ, for the local field fluctuations at the nucleus in the presence of a paramagnetic center is given by

$$\tau^{-1} = \tau_d^{-1} + \tau_p^{-1}$$

where τ_d is the time between proton jumps and the relaxation time of the paramagnetic center, τ_p, is only weakly temperature dependent. The low temperature behavior is accounted for if $\tau_p \ll \tau_d$. The data were corrected for the effect of the paramagnetic interaction and an activation energy for Motion B was then calculated from the variation of T_1 below its minimum to be 26.7 ± 1.0 kJ mole^{-1}.

Owing to the effects of Motion A on the T_1 data above 400 K it was impossible to locate the position of the T_1 minimum; however, the $T_{1\rho}$ data showed distinct minima and these were used to derive values of τ_c^0 for the motion. The best fit to the data shown in Fig. 2 is in terms of two motions characterized by the parameters shown in Table I. The solid lines in Fig. 2 represent the theoretical curves assuming BPP theory; the fit for Motion A is excellent showing the validity of BPP theory for this diffusion process. For Motion B the fit is also reasonable and is improved by correction of the theoretical values to allow for the effects of relaxation involving paramagnetic centers. This motion is unlikely to be of a diffusive nature and the application of BPP theory is less exact.

The variation of the second moment with temperature is shown in Fig. 5: the data recorded by Fourquet is shown for comparison and demonstrates good agreement in the common temperature range.

$HTaO_3$

Again the relaxation time/temperature behavior is best explained in terms of two

TABLE I

MOTIONAL PARAMETERS FOR $HNbO_3$

	Temperature range	E_a (kJ mole^{-1})	τ_c^0 (ps)
Motion A	>390 K	42.8 ± 0.4	30 ± 10
Motion B	200–310 K	26.7 ± 1.0	4 ± 1

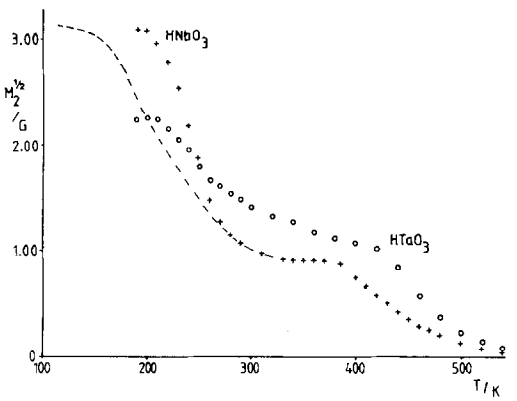

FIG. 5. Variation of the square root of the second moment with temperature for $HNbO_3$ (+) and $HTaO_3$ (O). Data recorded by Fourquet is shown as a broken line.

motions. However, it is more difficult to analyze the data for this material as proton diffusion occurs at temperatures near the limit of the available temperature range. However, the temperature variation of the T_2 and $T_{1\rho}$ data at the highest temperatures enabled a value of E_a of 52 ± 0.5 kJ mole^{-1} to be determined and a value of $\tau_c^0 = 27$ ps to be estimated. Motional parameters for Motion B were determined in a manner similar to that employed for $HNbO_3$ and a summary of the characteristic parameters for both proton motions in $HTaO_3$ is given in the Table II. The theoretical curves generated using these parameters are shown in Fig. 3; no correction has been made for the modulating effects of τ_p to the calculated data.

Alternating Current Conductivity

Conductivity measurements in the temperature range 470–570 K are shown in Fig. 3 for both compounds. A least-squares fit to the points yields values of the activation energy for diffusion of 49.0 ± 5 kJ mole^{-1} for $HNbO_3$ and 50.5 ± 4 kJ mole^{-1} for $HTaO_3$. These values are in fairly good agreement with those determined from the NMR data for Motion A.

Proton motion in these compounds can proceed by a series of hops between equivalent sites in the crystal. Of 24 otherwise identical oxygen atoms that occur in the unit cell only one-third are bonded to hydrogen with the formation of hydroxide groups. Proton diffusion can be visualized in terms of a mechanism involving protons hopping from one oxygen to another not already bonded to hydrogen.

The fall of the remaining second moment for both substances toward zero over the high-temperature range provides evidence for proton diffusion at these temperatures. The activation energies determined from the a.c. conductivity measurements in this same temperature range are in good agreement with those determined from NMR data. Values determined for the correlation times of $\sim 10^{-11}$ s are comparable to phonon frequencies.

Characteristic parameters for diffusion in these materials are in fair agreement with those found in the pyrochlore $HTaWO_6$ which also contains randomly distributed —OH groups and is nonmetallic (*13*). Diffusion in this compound is thought to occur via proton hops over a distance of ~1.7 Å and is characterized by $E_a = 26$ kJ mole^{-1} and $\tau_c^0 \sim 30$ ps.

The nature of the lower temperature Motion B is more uncertain. It could arise from a rotation of hydrogen about the M–O axis in HMO_3 which would be expected to remove part or all of the metal–hydrogen magnetic interaction. (The rigid lattice contribution to the second moment from this source is ~7 G^2 in $HNbO_3$ and ~1.0 G^2 in

TABLE II

MOTIONAL PARAMETERS FOR $HTaO_3$

	Temperature range	E_a (kJ mole^{-1})	τ_c^0 (ps)
Motion A	>420 K	52 ± 0.5	27 ± 8
Motion B	220–340 K	29.8 ± 1.2	1.9 ± 0.5

$HTaO_3$.) However, the observed change in the second moment of $HNbO_3$ of ~10 G^2 to ~1 G^2 in the relevant temperature range, 200–310 K, is too large to be accounted for entirely by this effect. The lower activation energies for Motion B in both materials suggest, though, that shorter proton hopping distances are involved than for the free proton diffusion of Motion A and the nature of this motion is localized.

Finally, it is possible to interpret the values determined for the rigid lattice second moment in terms of the structure of the materials. The value determined in this work for $HNbO_3$ of 9.1 ± 1.4 G^2 compares reasonably well with that determined by Fourquet using broad line measurements. Calculations based on a random distribution of protons after the elimination of contributions resulting from hydrogen atoms attached to the same oxygen atom lead to a value for M_2 of 11.3 G^2 in fair agreement with the experimental value. It is unnecessary to postulate, as did Fourquet (*4*), that $-OH_2$ groups are present. The experimental second moment for $HTaO_3$ of 5.2 ± 0.6 G^2 is in good agreement with the calculated value of 5.0 G^2 assuming the proton positions are those determined by neutron diffraction at room temperature (*5*).

Conclusion

Proton motion in both $HNbO_3$ and $HTaO_3$ can be interpreted in terms of two motions; a diffusive motion that occurs above ~400 K and a short-range motion occurring below room temperature.

Acknowledgments

We thank the AFSOR for financial support (Grant 83-0052) and one of us (M.T.W.) thanks the SERC for a research studentship. We also thank Dr. P. G. Bruce for assistance with the a.c. conductivity measurements.

References

1. C. E. Rice and J. L. Jackel, *J. Solid State Chem.* **41,** 308 (1982).
2. P. J. Wiseman and P. G. Dickens, *J. Solid State Chem.* **6,** 374 (1973).
3. P. G. Dickens and M. T. Weller, *J. Solid State Chem.* **48,** 407 (1983).
4. J. L. Fourquet, M. F. Renou, R. De Pape, H. Theveneau, P. P. Man, O. Lucas, and J. Pannettier, *Solid State Ionics* **9/10,** 1011 (1983).
5. M. T. Weller and P. G. Dickens, *J. Solid State Chem.* **58,** 164 (1985).
6. P. G. Dickens, D. J. Murphy, and T. K. Halstead, *J. Solid State Chem.* **6,** 370 (1973).
7. M. T. Weller and P. G. Dickens, *Solid State Ionics* **9/10,** 1081 (1983).
8. S. R. Hartmann and E. L. Hahn, *Phys. Rev.* **128,** 2042 (1962).
9. S. Meiboom and D. Gill, *Rev. Sci. Instr.* **29,** 688 (1958).
10. J. G. Powles and J. H. Strange, *Proc. Phys. Soc.* **82,** 6 (1963).
11. P. Mansfield, *Phys. Rev. A* **137,** 961 (1965).
12. N. Bloembergen, E. M. Purcell, and R. V. Pound, *Phys. Rev.* **73,** 679 (1948).
13. M. A. Butler and R. M. Biefeld, *Phys. Rev. B* **19,** 5455 (1981).